Synthesis of Molecular Brushes with Block Copolymer Side Chains Using Atom Transfer Radical Polymerization

Hans G. Börner, Kathryn Beers, and Krzysztof Matyjaszewski*

Center for Macromolecular Engineering, Department of Chemistry, Carnegie Mellon University, 4400 Fifth Avenue, Pittsburgh, Pennsylvania 15213

Sergei S. Sheiko*,† and Martin Möller*

Organische Chemie III/Makromolekulare Chemie, Universität Ulm, 89069 Ulm, Germany

Received January 2, 2001

ABSTRACT: Brush macromolecules having poly(*n*-butyl acrylate-*block*-styrene) and poly(styrene-*block*-*n*-butyl acrylate) side chains have been synthesized by the "grafting from" approach using atom transfer radical polymerization (ATRP). The molecular weights of the resulting polymers were characterized by gel permeation chromatography (GPC) using refractive index and multiangle light scattering detection. The block copolymer side chains were cleaved from the backbone and analyzed by GPC, confirming the synthesis of well-defined copolymer brushes. Visualization of individual molecules by atomic force microscopy (AFM) enabled analysis of the conformation and microstructure of the brush macromolecules on mica surface. The brushes with the p*n*BuA core were almost fully stretched, while the inverted structure with the pS core exhibited longitudinal contraction compared to the contour length of the main chain. In addition, the poly(*n*-butyl acrylate-*block*-styrene) brushes demonstrated a characteristic necklace morphology which was attributed to the interplay between the extension of the p*n*BuA core and microphase segregation of the pS tails.

Introduction

Recently there has been an increasing interest in densely grafted copolymers.[1−7] To better understand the structure−property relationship of these macromolecules, a series of well-defined polymers varying the nature of side chains, their chain length, architecture, and composition as well as the structure of polymer backbone are needed.

The synthesis of the densely grafted copolymers, molecular brushes that are also termed bottle brushes, can be accomplished through three routes:[8−15] "grafting through" (homopolymerization of macromonomers), "grafting onto" (attachment of side chains to the backbone), and "grafting from" (grafting side chains from the backbone). Various polymerization mechanisms, including cationic and anionic, have been employed for the synthesis of the densely grafted copolymers.

We have previously described the controlled synthesis of molecular brush copolymers by "grafting from" a macroinitiator using atom transfer radical polymerization (ATRP).[15−17] The macroinitiator was obtained by polymerization of 2-(trimethylsilyloxy)ethyl methacrylate (HEMA-TMS), followed by cleavage of the TMS protective groups and esterification with 2-bromopropionyl bromide to produce poly(2-(2-bromopropionyloxy)-ethyl methacrylate) (pBPEM) (Scheme 1A). This was used to initiate a controlled polymerization of several monomers from each repeat unit under ATRP conditions. The controlled radical polymerization allows for a variety of synthetic routes that enable synthesis of homo- and copolymers, statistical, gradient, and block copolymers followed by possible end functionalization.[18]

This article describes the extension of the "grafting from" approach toward densely grafted copolymers with block copolymer side chains (Schemes 1B and 2).

The resulting core/shell cylindrical molecules can be used for preparing nanoscopic channels, wormlike micelles, and other complex architectures. Here, we report the synthesis of brush molecules that consist of a soft poly(*n*-butyl acrylate) (p*n*BuA) core and a hard shell of polystyrene (pS) (Figure 1). We also prepared the inverted structures, consisting of pS core and p*n*BuA shell. The blocks have different glass transition temperatures defining their relative hardness/softness at the ambient temperature (−50 °C for p*n*BuA and 100 °C for pS).

Experimental Part

Materials. 2-(Trimethylsilyloxy)ethyl methacrylate (HEMA-TMS, 97.4% (GC)),[15,19] *n*-butyl acrylate (*n*BuA, Aldrich, 98%), and styrene (S, Aldrich, 99%) were stirred over calcium hydride for 2 days, distilled under vacuum (1×10^{-2} mbar), and stored at −15 °C under an inert gas atmosphere. Copper(I) bromide (Aldrich, 98%) was purified by steering over glacial acetic acid (Fisher Scientific), followed by filtration and washing of the solid three times with ethanol and twice with diethyl ether. The solid was dried under vacuum (1×10^{-2} mbar) for 2 days.[20] Copper(II) bromide (Aldrich, 99+%) was used as received. 4,4′-Di(5-nonyl)-2,2′-bipyridyne (dNbpy) was prepared as described previously.[21] All solvents and internal standards were used without further purification.

Measurements. Monomer conversion was determined using a Shimadzu GC 17A gas chromatograph equipped with a AO20ic autosampler and a FID detector using J&W Scientific 30 m DB608 column. Injector and detector temperatures were kept constant at 250 °C (conditions: butanone (internal standard)/*n*-butyl acrylate (monomer): start temperature 50 °C, isotherm 0 min, heating rate 30 °C/min, final temperature 160 °C, isotherm 0 min; toluene (internal standard)/styrene (monomer): start temperature 40 °C, isotherm 1 min, heating rate 20 °C/min, final temperature 130 °C, isotherm 0 min). The conversion was calculated by detecting the decrease of the monomer peak area relative to the standard peak area. GC measurements were repeated 4−7 times for each sample to reduce errors.

* To whom correspondence should be addressed.
† Current address: Department of Chemistry, University of North Carolina at Chapel Hill.

10.1021/ma010001r CCC: $20.00
Published on Web 05/17/2001

Scheme 1. Synthesis of the Macroinitiator (A) and "Grafting From" Approach to pBPEM-*graft*-(p*n*BuA-*Block*-pS) (B)

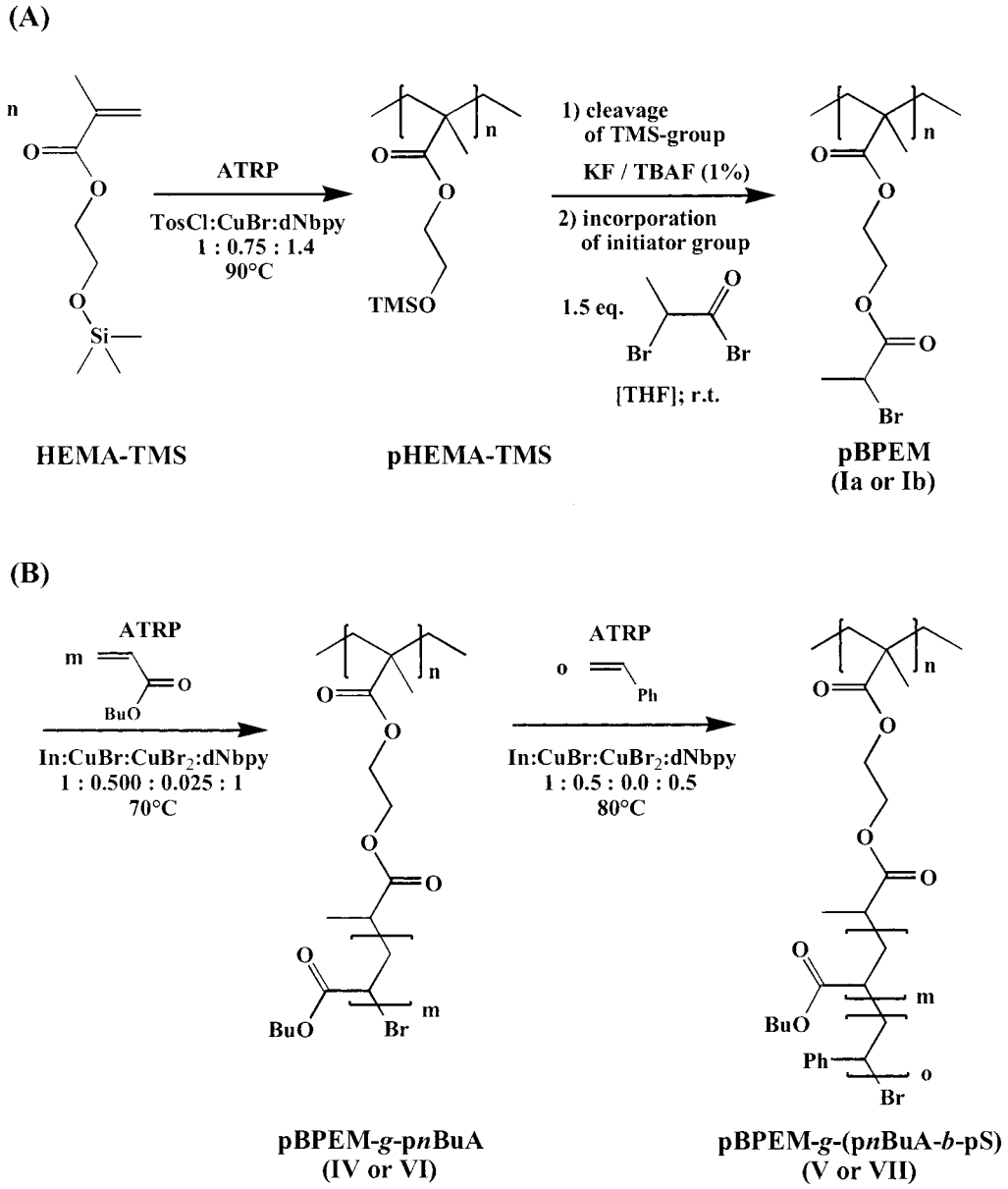

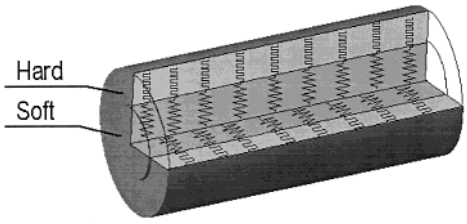

Figure 1. Idealized structure of the segment of cylindrical core/shell molecular brush.

Weight-average molecular weights were determined by gel permeation chromatography (GPC) equipped with Waters microstyragel columns (pore size 10^5, 10^4, and 10^3 Å) and three detection systems: a differential refractometer (Waters model 410), multiangle laser light-scattering (MALLS) detector (DAWN model F), a differential viscometer (Viscotek model H502), and GPC Win software. Measurements were conducted in THF (35 °C) at a flow rate of 1 mL/min. The setup was calibrated against low-polydispersity poly(methyl methacrylate) (pMMA) or polystyrene (pS) standards (PSS, Germany) with toluene as internal standard. The refractive index increment d*n*/d*c* was determined with an Otsuka Photal RM-102 differential refractometer. In addition to the GPC characterization, degrees of polymerization were estimated from conversion by assuming quantitative initiation for both macroinitiator and brush synthesis, $DP_{conv} = \Delta[M]/[I]_0$.

^{1}H NMR characterization was performed on a Bruker 300 MHz spectrometer. The measurements were carried out in chloroform-*d* or methylene chloride-d_2. The amount of incorporated monomer in *n*BuA/S copolymers was determined by ^{1}H NMR measurements by comparing the peak area ratio of characteristic signals for p*n*BuA (δ = 0.93 ppm, t, ^3J = 7.3 Hz, 3H, O−$(CH_2)_3$−CH_3 and δ = 4.00 ppm, bs, 2H, O−CH_2−CH_2−CH_3) and pS (δ = 7.23−6.10 ppm, m, 5H, Ar−H).

Atomic force micrographs were recorded with a Nanoscope IIIa instrument (Digital Instruments, St. Barbara, CA) operating in the tapping mode. The measurements were performed at ambient conditions (in air, 56% relative humidity, 27 °C) using Si cantilevers with a spring constant of ca. 50 N/m, a tip radius of 8 nm, and a resonance frequency of about 300 kHz. The set-point amplitude ratio was maintained at 0.9 to minimize the sample deformation induced by the tip. The samples for tapping mode SFM measurements were prepared by spin-casting on a rotating substrate at 2000 rpm of dilute solutions of brush molecules in chloroform.

A special software program was developed for the determination and analysis of the in-plane coordinates of the adsorbed molecules visualized by AFM. The coordinates of the molecular contour were determined by dragging a cursor along the contour and automatic recording the point coordinates. The program enabled statistical evaluation of different molecular dimensions, such as the contour length, the radius of gyration, the end-to-end distance, and the persistence length. The molecular dimensions were averaged for a large assembly of molecules (>200) to ensure accuracy within a statistical error of 5%.

Polymer Synthesis. Poly(HEMA-TMS) was prepared as described previously in the Supporting Information available to ref 15.

*(2-(2-Bromopropionyloxy)ethyl Methacrylate (pBPEM) (**Ia**).* PHEMA-TMS ($M_n = 1.01 \times 10^5$, $M_w/M_n = 1.12$) (9.9 g, assumed 49 mmol) was dissolved in 125 mL of dry THF under nitrogen. Potassium fluoride (2.85 g, 49 mmol) was added followed by slow addition of 0.5 mL of tetrabutylammonium fluoride (1 M in THF; 0.5 mmol) and then dropwise addition of 7.75 mL of 2-bromopropionyl bromide (74 mmol) over the course of 15 min. The reaction mixture was stirred at room temperature for 4 h, exposed to air, precipitated into methanol/ice (50/50 v/v), dissolved in 200 mL of $CHCl_3$, and filtered through an activated alumina column (basic). The polymer was reprecipitated three times in hexanes and dried in a vacuum oven at 25 °C for 24 h. 8.7 g of pBPEM was obtained (83% yield). Complete conversion was determined by ^{1}H NMR (absence of TMS − resonance $\delta = 0.2$ ppm (9H, bs, $(H_3C)_3Si-$)).

^{1}H NMR (300 MHz, $CDCl_3$, δ in ppm): 4.52 (1H, quart., $J = 6.8$ Hz, Br−C*H*−CH_3); 4.36 (2H, bs, −O−CH_2−C*H*$_2$−O−CO−CH−Br); 4.15 (2H, bs, −O−C*H*$_2$−CH_2−O−CO−CH−Br); 1.82 (overlapped, d, $J = 6.8$ Hz, Br−CH−C*H*$_3$); 2.21−1.44 (overlapped, m, C*H*$_2$−C−CH_3); 1.22, 1.05, 0.94 (3H, 3 × bs, CH_2−C−C*H*$_3$).

Two pBPEM macrointiators (**Ia** and **Ib**) that differ in the degree of polymerization were prepared. The molecular weights and the degree of polymerizations (DP) of the macroinitiators were determined by GPC-MALLS as $M_n = 1.36 \times 10^5$, $M_w/M_n = 1.16$, and $DP_n = 514$ for macroinitiator **Ia** and $M_n = 1.5 \times 10^5$, $M_w/M_n = 1.18$, and $DP_n = 567$ for macroinitiator **Ib**. Similar values were obtained using universal calibration based on viscosity measurements in GPC.

*pBPEM-graft-pS (**II**).* In a 100 mL Schlenk flask, pBPEM (**Ia**) (0.3 g, 1.14 mmol initiator centers), $CuBr_2$ (0.0076 g, 0.034 mmol), and dNbpy (0.371 g, 0.909 mmol) were purged three times with inert gas. Afterward, deoxygenated styrene (70.9 g, 78.4 mL, 0.68 mol) and anisole (5 mL, 6 vol %) were added, and the reaction mixture was degassed via three freeze−pump−thaw cycles. After stirring for 1 h at room temperature (rt), CuBr (0.065 g, 0.45 mmol) was added, an initial sample was taken, and the flask was placed in a thermostated oil bath at 80 °C. During the polymerization, samples were removed to analyze conversion by GC using anisole as the internal standard.

The polymerization was stopped after 14.3 h at 5.2% conversion (GC) by cooling to rt and opening the flask to air. GPC-MALLS was used to analyze the molecular weight and the polydispersity ($M_n = 1.49 \times 10^6$, $M_w/M_n = 1.23$). The GPC samples were not precipitated; rather they were diluted with THF, passed through a short alumina column to remove the copper catalyst, and analyzed directly in THF against pS standards. The polymer was purified by distilling off both the solvent and the monomer under vacuum, dissolving the crude polymer in chloroform (about 100 mL), passing it through a column (2 cm × 13 cm) of alumina, and reprecipitating it into methanol (1000 mL). Yield: 3.38 g of isolated polymer (4.3% monomer conversion).

*pBPEM-graft-(pS-block-pnBuA) (**III**).* In a 100 mL Schlenk flask, pBPEM-*graft*-pS (**II**) (2.5 g, 0.74 mmol initiator groups[22]), dNbpy (0.301 g, 0.74 mmol), and copper(II) bromide (0.0025 g, 0.011 mmol) were purged three times with inert gas. Subsequently, deoxygenated *n*-butyl acrylate (37.8 g, 42.1 mL, 29.5 mmol) and butanone (MEK, 42.1 mL, 50 vol %) were added, and the reaction mixture was degassed by three freeze−pump−thaw cycles. After stirring at rt for 2 h, CuBr (0.0529 g, 0.369 mmol) was added, an initial sample was taken, and the flask was placed in a thermostated oil bath at 80 °C. The conversion was followed by GC analysis using MEK as the internal standard.

The polymerization was stopped at 2% conversion (GC) after 20 h by cooling the reaction mixture to rt and afterward exposing it to air. A small sample was analyzed after catalyst removal by GPC-MALLS ($M_n = 1.98 \times 10^6$, $M_w/M_n = 1.26$). Purification following the procedure described above gave 3.44 g of isolated polymer (2.5% monomer conversion). Copolymer composition was determined by ^{1}H NMR (300 MHz, CD_2Cl_2, proton resonances used for integration were given in the method section); pS:p*n*BuA = 29:8.

*pBPEM-graft-pnBuA (**IV**).* In a 100 mL Schlenk flask pBPEM (**Ia**) (0.3 g, 1.14 mmol initiator centers), $CuBr_2$ (0.0063 g, 0.028 mmol) and dNbpy (0.463 g, 1.14 mmol) were purged three times with inert gas. Deoxygenated *n*BuA (58.5 g, 65.14 mL, 0.46 mol) and MEK (3 mL, 4 vol %) were then added, and the reaction mixture was degassed by three freeze−pump−thaw cycles. After stirring for 1 h at rt, CuBr (0.082 g, 0.568 mmol) was added, an initial sample was taken, and the flask was placed in a thermostated oil bath at 70 °C. During the polymerization, samples were removed to analyze conversion by GC using MEK as the internal standard. The polymerization was stopped at 3.5% conversion (GC) after 12 h by cooling to rt and opening the flask to air. GPC-MALLS analysis was proceeded with a crude polymer sample ($M_n = 0.97 \times 10^6$, $M_w/M_n = 1.22$), and after purification of the polymer following the procedure described above (precipitation in methanol with 20 vol % water), 2.72 g was obtained as isolated polymer (4.3% monomer conversion).

Using the same procedure, pBPEM-*graft*-p*n*BuA (**VI**) was prepared by grafting *n*BuA from pBPEM (**Ib**). The polymerization was stopped after 26 h at 14% (GC) monomer conversion (12% gravimetry). $M_n = 3.4 \times 10^6$ and $M_w/M_n = 1.38$ were determined by GPC-MALLS analysis.

*pBPEM-graft-(pnBuA-block-pS) (**V**).* In a 25 mL Schlenk flask pBPEM-*graft*-p*n*BuA (**IV**) (0.22 g, 0.09 mmol initiator centers[22]) and dNbpy (0.0184 g, 0.045 mmol) were purged three times with inert gas. Deoxygenated styrene (3.75 g, 4.14 mL, 36.0 mmol) and toluene (4.14 mL, 50 vol %) were added, and the reaction mixture was degassed by three freeze−pump−thaw cycles. After stirring for 2 h at rt, CuBr (0.0065 g, 0.045 mmol) was added, an initial sample was taken, and the flask was placed in a thermostated oil bath at 80 °C. During the polymerization, samples were removed to analyze conversion by GC using toluene as the internal standard.

The polymerization was stopped at 2.8% conversion (GC) after 8.7 h by cooling the reaction mixture to rt and afterward exposing it to air. GPC-MALLS analysis was followed with a nonprecipitated sample ($M_n = 1.49 \times 10^6$, $M_w/M_n = 1.24$), and after purification of the polymer following the procedure described above (precipitation in methanol) 0.28 g of isolated polymer was obtained (1.5% monomer conversion). Copolymer composition was determined by ^{1}H NMR (300 MHz, CD_2Cl_2, proton resonances used for integration were given in the method section); p*n*BuA:pS = 16:7.

Following the same procedure, pBPEM-*graft*-(p*n*BuA-*block*-pS) (**VII**) was synthesized by side chain extension of **VI**. The polymerization was stopped after 22 h at 9% monomer conversion (GC) and 8% by gravimetry. $M_n = 5.4 \times 10^6$ and $M_w/M_n = 1.28$ were determined by GPC-MALLS analysis. Copolymer composition was determined by ^{1}H NMR (300 MHz, CD_2Cl_2, proton resonances used for integration were given in the method section); p*n*BuA:pS = 52:30.

Graft Copolymer Solvolysis (General Procedure). 0.05 g of polymer (e.g., **VI** or **VII**) was dissolved in 3 mL of THF in a 25 mL flask. *n*-Butanol was added until the polymer started to precipitate (approximately 15 mL of *n*-butanol). After adding 4 drops of concentrated sulfuric acid, the mixture was heated to 95−100 °C for 7 days. The solvent was removed under vacuum (1×10^{-2} mbar), and the remaining polymer was dissolved in chloroform. After an extraction with a small amount

Table 1. Syntheses of pBPEM-*graft*-(pS-*block*-p*n*BuA)[h,i]

	condition (time, h)	$M_w \times 10^{-6}$ [b,j]	M_w/M_n [j]	$M_p \times 10^{-6}$ [c]	DP_n [d]	DP_p [e]	DP [g]	conversion (DP_{conv}) GC	gravimetry	av
pBPEM-*g*-pS **(II)**[a]	A (14.3)	1.83	1.23	1.42	29	25	27 ± 2	5.2% (31)	4.3% (26)	(29 ± 3)
pBPEM-*g*-(pS-*b*-p*n*BuA) **(III)**[a]	B (20)	2.49	1.26	2.01	11	7	9 ± 2[f]	2.0% (8)	2.5% (10)	(9 ± 2)

[a] Used macroinitiator pBPEM (**Ia**) ($M_n = 1.36 \times 10^5$ g/mol, $M_w/M_n = 1.16$, and the peak value $M_p = 1.15 \times 10^5$ g/mol). [b] THF, MALLS detector, d*n*/d*c*(**II**) = 0.176 ± 0.002 mL/g, d*n*/d*c*(**III**) = 0.134 ± 0.002 mL/g. [c] Peak value of the molecular weight distribution of the brushes. [d] $DP_n = [(M_n - M_n^{MI})M_0]/M_n^{MI}m_0$, where M_0 = 265 g/mol − molecular weight of the macroinitiator monomer unit, m_0 is the molecular weight of the side chain monomer unit: styrene (104 g/mol) or *n*-butyl acrylate (128 g/mol), and M_n^{MI} is the number-average molecular weight of the macroinitiator. [e] $DP_p = [(M_n - M_n^{MI})M_0]/M_p^{MI}m_0$, where M_p and M_p^{MI} are thepeak value of the molecular weight distribution of the brush and macroinitiator,[a] respectively. [f] The DP values for polymer **III** correspond to the p*n*BuA block. [g] Average degree of polymerization of the side chains DP = (DP_n + DP_p)/2. [h] $[S]_0$:$[In]_0$:$[Cu^I]_0$:$[Cu^{II}]_0$:[dNbpy]$_0$:[anisole]$_0$ = [600]:[1]:[0.40]:[0.03]:[0.8]:[6 vol %]. [i] $[n\text{BuA}]_0$:$[In]_0$:$[Cu^I]_0$:$[Cu^{II}]_0$:[dNbpy]$_0$:[MEK]$_0$ = [400]:[1]:[0.500]:[0.015]:[1]:[50 vol %]. [j] Integrated over the main peak (approximately 96−98 area %).

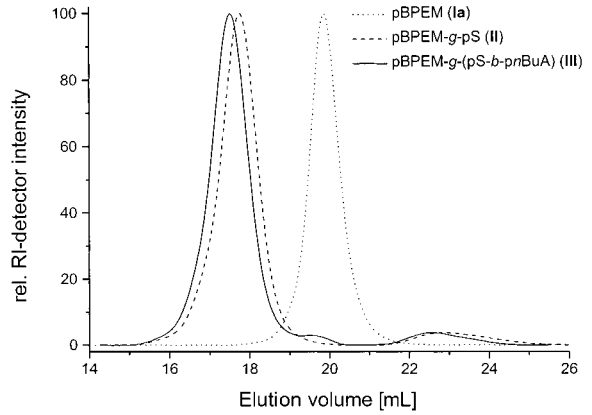

Figure 2. GPC traces of the subsequent synthesis of pBPEM-*graft*-(pS-*block*-p*n*BuA).

of water, the organic phase was isolated, the solvent was distilled off, and the remaining polymer was analyzed by GPC.

To determine the extent of hydrolysis, the number distribution of the GPC trace of the hydrolysis products was calculated. By comparison of the integrated area of the low molecular weight fraction (cleaved side chains) with the high molecular weight fraction, the percentage of cleaved side chains was calculated.

Results and Discussion

Synthesis of Densely Grafted Copolymers with Block Copolymer Side Chains. A variety of densely grafted copolymers can be prepared using the "grafting from" method by controlled atom transfer radical polymerization (ATRP).[15,16] Since the initiating groups remain at the ends of the grafted side chains, it is possible to extend the side chains in a well-defined manner.

pBPEM-graft-(pS-block-pnBuA). The styrene polymerization was initiated with a well-defined pBPEM macroinitiator, **Ia** ($M_n = 1.36 \times 10^5$, $M_w/M_n = 1.16$). This reaction resulted in a pBPEM-*graft*-polystyrene copolymer (**II**) that shows a symmetrical shift of the GPC trace after 14.3 h (Figure 2). The polydispersity $M_w/M_n = 1.23$ of the synthesized molecular brushes is very close to that of the macroinitiator. The polydispersity of the brush is merely determined by the polydispersity of the backbone.[23] The slight increase from $M_w/M_n = 1.16$ to $M_w/M_n = 1.23$ and the appearance of a small oligomer side peak (3 area %) suggest that some side reactions occur. There are three possible reasons for the appearance of oligomeric side products. The first is that some of the remaining low molecular weight halides used during the pBPEM synthesis can act as ATRP initiators. These halides might be unpolymerized HEMA-TMS that is transesterified to free BPEM or 2-bromopropionic acid derivatives, which are not completely removed after the transesterfication. The second possibility is the spontaneous cleavage of some side chains due to strong intramolecular repulsion between the densely grafted side chains. Finally, a secondary initiation process may be possible via either a thermal self-initiation of styrene or by the copper-catalyzed generation of new chains in the presence of trace amounts of oxygen.[24] Further mechanistic investigations into this last possibility are in progress, and the results will be published elsewhere.

The narrow and monomodal molecular weight distribution enabled evaluation of the number-average degree of polymerization of the side chains DP_n from the independently determined molecular weights of the macroinitiator and the brush. In addition to DP_n, the peak values of the brush and macroinitiator molecular weight distributions were used to calculate DP_p of the side chains. Thus, the DP_p would correspond to the largest fraction of the macromolecules. Assuming that the length and the length distribution of the side chains do not depend on the length of the backbone, the DP_n and DP_p should give the same values. However, there should be some discrepancy due to the difference in detection of high and low molecular weight species by GPC-MALLS. The results are summarized in Table 1. The average degree of polymerization of the side chains, DP = 27 ± 2, is in agreement with DP_{conv} = 29 ± 3, which was determined from the monomer conversion by both GC and gravimetry.

The polystyrene graft copolymer **II** was isolated and used as a macroinitiator for the polymerization of *n*-butyl acrylate, which resulted in poly(styrene-*block*-*n*-butyl acrylate) brush **III**. Figure 2 shows a shift of the main peak and a small increase in the polydispersity (Table 1). There is no detectable brush-coupling product, indicating a controlled polymerization reaction. The reaction was stopped at 2% conversion after 20 h. The degree of polymerization of the *n*BuA block, $DP_{n\text{BuA}}$ = 9 ± 3, was obtained from the GPC-MALLS analysis and corresponds well to $DP_{conv,n\text{BuA}}$ = 9 ± 2 from the monomer conversion data. The resulting block ratio pS:p*n*BuA = 29:9 was also confirmed by ^{1}H NMR measurements, which showed that the incorporated monomer ratio between S and *n*BuA was 29:8.

pBPEM-graft-(pnBuA-block-pS). Figure 3 shows the GPC traces of the polymer precursor (pBPEM (**Ia**), intermediate pBPEM-*graft*-p*n*BuA (**IV**), and the end product (pBPEM-*graft*-(p*n*BuA-*block*-pS) (**V**)).

The *n*BuA polymerization using **Ia** as macroinitiator occurs in a controlled way (Table 2). The increase of the molecular weight of the resulting graft copolymer **IV** is

Table 2. Synthesis of PBPEM-*graft*-(p*n*BuA-*block*-pS)[g,h]

	condition (time, h)	$M_w \times 10^{-6}$ [b,i]	M_w/M_n [i]	$M_p \times 10^{-6}$ [c]	DP_n [d]	DP_p [e]	DP [f]	conversion ($DP_{conv.}$) GC	gravimetry	av
pBPEM-*g*-p*n*BuA (**IV**)[a]	A (12)	1.18	1.22	0.94	15	15	15 ± 2	3.5% (14)	4.3% (17)	(16 ± 2)
pBPEM-*g*-(p*n*BuA-*b*-pS) (**V**)[a]	B (8.7)	1.85	1.24	1.48	12	7	9 ± 3	2.8% (11)	1.5% (6)	(9 ± 3)
pBPEM-*g*-p*n*BuA (**VI**)[a]	A (26)	4.70	1.38	3.40	49	51	50 ± 1	14.0% (56)	12.0% (48)	(52 ± 4)
pBPEM-*g*-(p*n*BuA-*b*-pS) (**VII**)[a]	B (22)	6.90	1.28	5.40	29	38	34 ± 4	9.0% (36)	8.0% (32)	(34 ± 3)

[a] Macroinitiator **Ia** was used for **IV** and **V**: pBPEM ($M_n = 1.36 \times 10^5$ g/mol; $M_w/M_n = 1.16$, and the peak value $M_p = 1.15 \times 10^5$ g/mol) macroinitiator **Ib** was used for **VI** and **VII**: pBPEM ($M_n = 1.5 \times 10^5$ g/mol; $M_w/M_n = 1.18$; $M_p = 1.33 \times 10^5$ g/mol). [b] THF, MALLS detector, d*n*/d*c*(**IV**, **VI**) = 0.069 ± 0.002 mL/g, d*n*/d*c*(**V, VII**) = 0.089 ± 0.002 mL/g. [c−f] See the corresponding comments in Table 1. [g] $[n\text{BuA}]_0:[\text{In}]_0:[\text{Cu}^{\text{I}}]_0:[\text{Cu}^{\text{II}}]_0:[\text{dNbpy}]_0:[\text{MEK}]_0 = [400]:[1]:[0.500]:[0.025]:[1]:[4$ vol %]. [h] $[\text{S}]_0:[\text{In}]_0:[\text{Cu}^{\text{I}}]_0:[\text{Cu}^{\text{II}}]_0:[\text{dNbpy}]_0:[\text{Toluene}]_0 = [400]:[1]:[0.5]:[0]:[0.5]:[50$ vol %]. [i] Integrated over the main peak (approximately 98−96 area %).

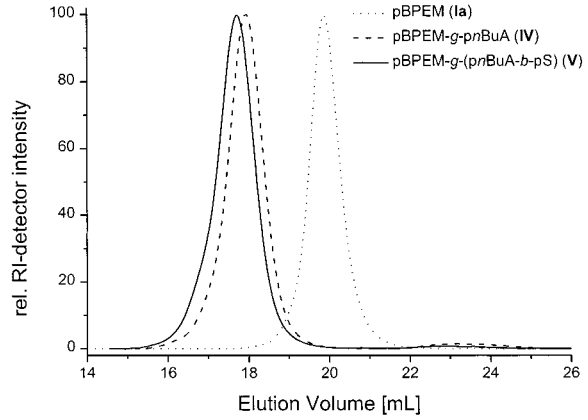

Figure 3. GPC traces of the subsequent synthesis of pBPEM-*graft*-(p*n*BuA-*block*-pS).

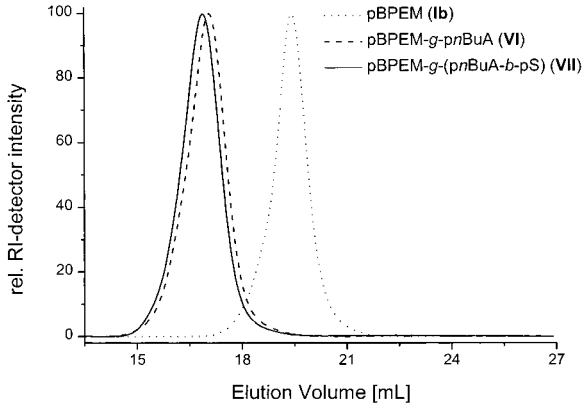

Figure 4. GPC traces of the subsequent synthesis of pBPEM-*graft*-(p*n*BuA-*block*-pS) before side-chain cleavage.

Scheme 2. General Approach to Graft Copolymers with Block Copolymer Side Chains

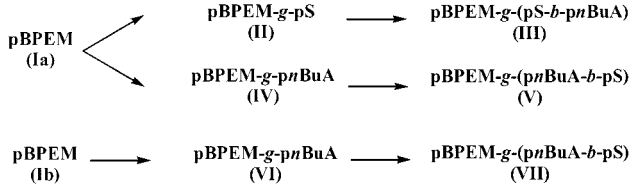

Scheme 3. Side Chain Cleavage of Molecular Brushes

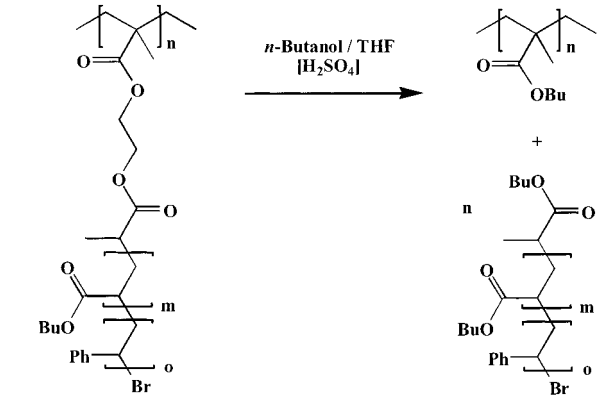

shown by the shift in the GPC trace (Figure 3). The molecular weight distribution is symmetric and monomodal ($M_w = 1.18 \times 10^6$, $M_w/M_n = 1.22$). This allowed precise evaluation of the number-average degree of polymerization of the side chains $DP_n = 15$, which was consistent with the average degree of polymerization $DP_{conv} = 16 \pm 2$ from the monomer conversion data.

The isolated p*n*BuA-brush (**IV**) was used as a macroinitiator for a styrene block copolymerization (Table 2). After 8.7 h, the reaction reached 2.8% conversion. The GPC trace of **V** is monomodal and shows no evidence of brush coupling products. The p*n*BuA side chain extension with styrene occurs in a controlled manner based on the fact that the GPC traces shift entirely toward higher molecular weight while remaining symmetric, and no brush coupling reactions could be detected. The polydispersity broadens slightly from **IV** to **V**. Calculations based on the GPC-MALLS analysis ($M_w = 1.85 \times 10^6$, $M_w/M_n = 1.24$) resulted in a degree of polymerization of the polystyrene block $DP_{pS} = 9 \pm 3$ that corresponded to $DP_{conv} = 9 \pm 3$ fairly well. Also, ^{1}H NMR measurements of the composition of **V** gave a p*n*BuA:pS ratio of about 16 to 7, which agrees well with the values based on monomer conversion (p*n*BuA:pS = 16:9).

Analysis of the Grafted Side Chains. The grafted side chains were cleaved from the backbone to determine their uniformity. The cleavage was carried out on molecular brushes with p*n*BuA (**VI**) and p*n*BuA-*block*-pS (**VII**) side chains, which were prepared from macroinitiator **Ib** ($M_n = 1.5 \times 10^5$, $M_w/M_n = 1.18$). To avoid altering the results fractionation needed to remove the oligomeric impurities from brush **II**/**III** or **IV**/**V**, brush samples (**VI**/**VII**) were chosen in which the oligomers were not present (Figure 4, Table 2). The side chains were cleaved using acid-catalyzed transesterfication in *n*-butanol to ensure that the *n*-butyl ester groups of the p*n*BuA- and the p*n*BuA-*block*-pS side chains remained intact during this step (Scheme 3).

As shown in Figure 5, the peak of the pBPEM-*graft*-(p*n*BuA-*block*-pS) (**VII**) copolymer disappeared during cleavage reaction. In its place, a low and a high molecular weight fraction appeared, which correspond to the cleaved side chains and to a small fraction of cross-linked chains, respectively. The amount of cross-

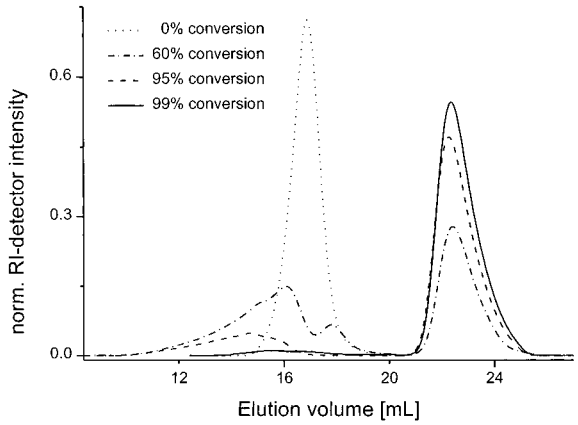

Figure 5. GPC traces of solvolysis of pBPEM-*graft*-(p*n*BuA-*block*-pS) (**VII)** in *n*-butanol (area normalized curves).

Table 3. GPC Characterization of the Brush Side Chains Cleaved by Butanolysis

	react. time (days)	conv (%)	M_n[a,b]	M_w/M_n[a]	side chain ($M_{n,calc}$)
pBPEM-*g*-p*n*BuA (**VI**)	7	99	6500	1.21	pnBuA (6660 ± 510)
pBPEM-*g*-(p*n*BuA-*b*-pS) (**VII**)	1	60	10 000	1.22	pS + pnBuA (10200 ± 720)
	4	95	10 500	1.22	
	7	99	9600	1.23	

[a] THF, RI detector, pMMA standards. [b] Baseline-separated low molecular weight peak.

linked material progressively disappears, indicating that the cleavage of the side chains from the cross-linked material also takes place. Samples taken during the cleavage contain a very similar low molecular weight fraction, as confirmed by GPC analyses (Table 3). This indicates that there is no preference for the cleavage of smaller or larger side chains. After cleavage of 99% of the side chains (calculated by comparison of peak areas of the number distribution), the low molecular weight fraction has symmetrical GPC traces, the number-average molecular weight is $M_n = 9600$, and the polydispersity is $M_w/M_n = 1.23$. The molecular weight corresponds to the block lengths of the side chains predicted on the basis of the conversion ($DP_{conv,pnBuA} = 52$; $DP_{conv,pS} = 34$):

$$M_{n,calc} = 128.17 \text{ g/mol} \times DP_{conv,pnBuA} + 104.15 \text{ g/mol} \times DP_{conv,pS} = 10200 \pm 720 \text{ g/mol}$$

Following the same procedure, the side chains of the p*n*BuA-brush (**VI**), which was used as a macroinitiator to synthesize **VII**, were cleaved from the backbone. After 99% conversion a low molecular weight fraction ($M_n = 6500$, $M_w/M_n = 1.21$) was detected in the GPC. The molecular weight of the low molecular weight fraction corresponds to that of the side chains, which was determined from the monomer conversion $M_{n,calc} = 128.17$ g/mol × $DP_{conv,pnBuA} = 6660 \pm 510$ g/mol, where $DP_{conv,pnBuA} = 52$ (Table 3).

As shown in Figure 6, the GPC traces of the cleaved p*n*BuA-side chains do not have any significant tailing toward low molecular weight. The entire distribution of the side chains cleaved from **VII** shifts toward higher molecular weight and remains monomodal. This indicates a controlled extension of the p*n*BuA-side chains with pS and no significant amount of intramolecular side chain coupling that should result in a bimodal side chain distribution ($M_{p,sc} + 2M_{p,sc}$). The side chain compositions, which were obtained from the cleavage experiment, were consistent with the corresponding data from GPC-MALLS measurements (Table 2).

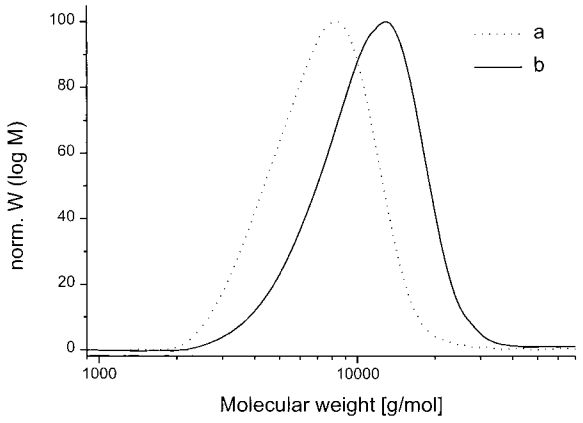

Figure 6. GPC traces of the cleaved side chains: (a) side chains form pBPEM-*graft*-(p*n*BuA) (**VI**); (b) side chain from pBPEM-*graft*-(p*n*BuA-*block*-pS) (**VII**).

In both side-chain cleavage experiments the remaining backbone polymer cannot be detected in the GPC traces. This is plausibly due to the low proportion of backbone with respect to side chains, which can be calculated as 2.4 wt % (**VI**) and 1.5 wt % (**VII**), assuming a complete transesterfication of the backbone polymer to poly(*n*-butyl methacrylate).

The results show that the "grafting from" reaction using the $CuBr/(dNbpy)_2$ catalytic system leads to a slow but well-controlled polymerization reaction. This also allows well-defined block copolymer side chains to be prepared from brush-type macromolecules with a low polydispersity.

Atomic Force Microscopy (AFM) Characterizations. Dilute solutions of the synthesized polymers were spin-cast on mica to prepare monomolecular films for AFM studies. Figure 7 shows AFM micrographs of pBPEM macroinitiator **Ia** (Figure 7a) and of three different molecular brushes that were prepared from this macroinitiator, i.e., p*n*BuA homopolymer brushes **IV** (Figure 7b), p*n*BuA-*b*-pS block copolymer brushes **V** (Figure 7c), and the inverted brushes with pS-*b*-p*n*BuA block copolymer side chains **III** (Figure 7d). In all cases, AFM revealed individual wormlike molecules lying flat on the substrate. The pictorial resolution of the chain ends allowed direct measurement of the molecular length for a large ensemble of ca. 200 molecules. The number-average as well as the weight-average length of brush molecules is depicted in Table 4. For polymers **Ia**, **III**, **IV**, and **V**, the length distribution L_w/L_n ranged between 1.1 and 1.2, which agrees well with the molecular weight distribution from MALLS measurements (Tables 1 and 2). To evaluate the contraction of the backbone relative to the contour length of the fully extended main chain, the length of the brush molecules per monomer unit of the backbone, l_m, was calculated and compared to $l_{max} = 0.25$ nm for the all-trans conformation of an aliphatic chain. The monomer length was determined as $l_m = L_n/DP_n$, where L_n is the number-average length of the adsorbed molecules from AFM micrographs and DP_n is the number-average degree of polymerization of the main chain, which was measured

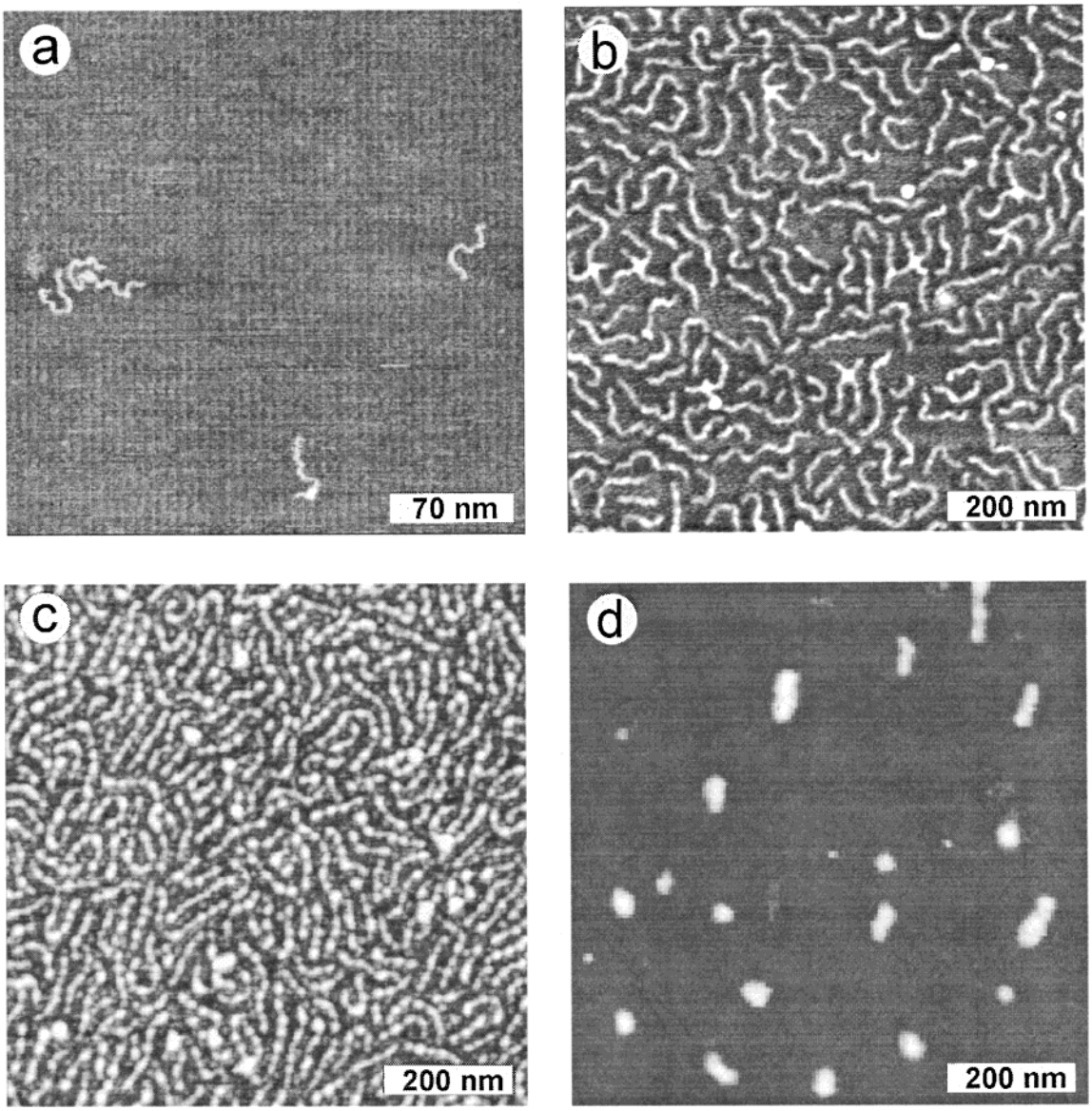

Figure 7. AFM micrographs of four different polymers adsorbed on mica: (a) single molecules of macroinitiator **Ia**; (b) monolayer of homopolymer pBPEM-*graft*-p*n*BuA brush **IV**; (c) monolayer of pBPEM-*graft*-(p*n*BuA-*block*-pS) brush **V**; (d) single molecules of pBPEM-*graft*-(pS-*block*-p*n*BuA) brush **III**. The length scale in a is much smaller than in (b)−(d).

Table 4. Molecular Dimensions from AFM Micrographs in Figure 7 (Spin-Casting from Chloroform, 2000 rpm, Mica, Rotating Substrate)

sample[a]	L_n (nm)[b]	L_w (nm)[b]	L_w/L_n[b]	l_m (nm)	D, nm[c]
pBPEM-*g*-p*n*BuA (**IV**)	113	126	1.12	0.22 ± 0.01	30 ± 2
pBPEM-*g*-(p*n*BuA-*b*-pS) (**V**)	105	119	1.13	0.20 ± 0.01	25 ± 2
pBPEM-*g*-(pS-*b*-p*n*BuA) (**III**)	83	95	1.15	0.16	na[d]

[a] Macroinitiator **Ia** was used for **III**, **IV**, and **V**: pBPEM (DP_n = 514). [b] The number- and weight-average length of brush molecules were evaluated for an assemble of ca. 200 molecules. [c] The distance between brush molecules in the dense monolayers was measured perpendicular to the molecular contour and averaged for more than 100 molecules. [d] Resolution of individual molecules of brush **III** was hindered by strong overlapping of macromolecules within a dense monolayer.

independently by GPC-MALLS analysis of the used pBPEM macroinitiator. For p*n*BuA brush **IV**, the length l_m = 0.22 nm indicates that the backbone is almost completely stretched. This is the result of strong interaction between the polar *n*BuA monomeric units and the polar mica substrate. In agreement with previous results,[7] the entropic elasticity of the tightly adsorbed side chains extends the backbone. The pBPEM-*g*-(p*n*-BuA-*b*-pS) brush **V** with p*n*BuA core and pS shell also extends to l_m = 0.20 nm. In contrast, the inverted structure, i.e., pBPEM-*g*-(pS-*b*-p*n*BuA) brush **III** with the pS core and p*n*BuA shell, contracts significantly (l_m = 0.16 nm) compared to the fully extended main chain. The axial contraction is consistent with the more globular morphology of the brush molecules in Figure 7d compared to those in Figure 7b,c.

Comparison of the micrographs in Figure 7c and Figure 7b indicates that the molecular morphologies of the block copolymer and homopolymer brushes, respectively, are significantly different. In contrast to the smooth contour of the p*n*BuA brushes, the diameter along the backbone of the copolymer molecules in Figure 7c has periodic undulations. To exclude the effect of neighbors in the dense monolayers, single macromolecules were prepared and visualized by AFM. The two micrographs in Figure 8a,b show the high-resolution

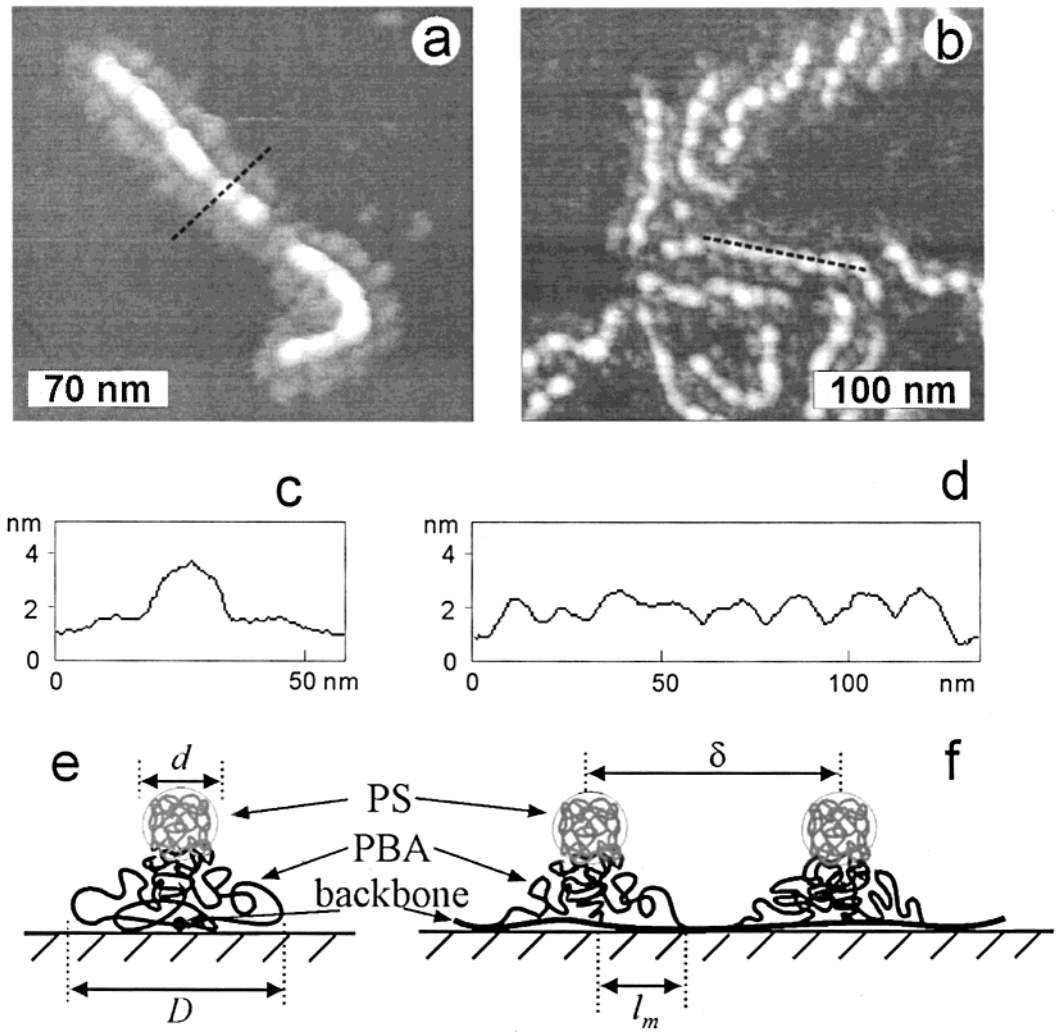

Figure 8. AFM micrographs of single molecules of pBPEM-*graft*-(p*n*BuA-*block*-pS) brushes **VII** (a) and **V** (b). The cross-sectional profiles (c) and (d) were drawn perpendicular and parallel to the molecular contour along the dot lines in (a) and (b). The corresponding scheme illustrates the necklace morphology upon looking at the molecule from the edge (e) and from the side (f).

structure of pBPEM-*g*-(p*n*BuA-*b*-pS) copolymer brushes **VII** and **V**, their undulating backbones, and surrounding thin films. The two cross-sectional profiles in parts d and c of Figure 8 were recorded along the molecular backbone and perpendicular to it, respectively. The following molecular parameters were extracted from the profiles: the height of the undulations 2.5 ± 0.5 nm, the depth of the dimple between the undulations 1.0 ± 0.2 nm, and the thickness of film around the backbone 0.5 ± 0.1 nm. These values may be underestimated due to the indentation of the AFM tip. After deconvolution of the tip radius ($R \sim 8$ nm) from the profiles, one obtains a necklace-like morphology, in which small globuli with the diameter $d = 5 \pm 1$ nm are separated by the distance $\delta = 15 \pm 2$ nm. A tentative interpretation of the undulations is presented in Figure 8e,f. In contrast to the homopolymer brushes, the pS tails in the block copolymer brushes tend to aggregate in order to reduce the interfacial energy between the pS and p*n*BuA blocks as well as between the pS and air. While aggregation occurs, the p*n*BuA chain fragments remain tightly adsorbed to the substrate as illustrated by the edge view in Figure 8e and by the side view in Figure 8f. This interpretation is also consistent with the intermolecular distance *D*, which was measured for the densely packed monolayers in Figure 7b,c. Table 4 shows that brushes **V** with the longer p*n*BuA-*b*-pS chains in Figure 7c are separated by a smaller distance of 25 nm than the *n*BuA brushes **IV** in Figure 7b, which are separated by $D = 30$ nm. This difference can be explained by raising and aggregation of the pS tails above the substrate plane as shown in Figure 8e.

There are two ways to determine the aggregation number Γ from AFM images. First, one can simply divide the undulations periodicity by the monomer length l_m, $\Gamma = \delta/l_m$. This method gave $\Gamma = 75 \pm 15$, which corresponds to 75 side chains whose pS tails are aggregated into one globule. The second method is based on the three-dimensional structure of the undulated molecules observed by AFM. Here, the aggregation number can be calculated as $\Gamma = V\rho N_A/M_{pS}$, where $V = \pi d^3/6$ is the globule volume, $\rho = 1$ g/cm^3 is the density of pS, $N_A = 6.022 \times 10^{23}$ mol^{-1} is Avogadro's number, and $M_{pS} = 936$ g/mol is the molecular mass of the pS tail in polymer **V** from Table 2. This method is less accurate since the AFM tip deforms the molecular structure and because of the unknown geometry and composition of the globuli in Figure 8a,b. Nevertheless, the obtained $\Gamma = 54 \pm 30$ is consistent within the estimated uncertainties to the more accurate value obtained from the undulations periodicity.

To summarize, the interplay between (i) stretching of the backbone, which is caused by extension of the adsorbed p*n*BuA blocks, and (ii) segregation of the pS

blocks, which are incompatible with their p*n*BuA counterparts, resulted in a necklace morphology, in which the pS globuli are separated by the extended p*n*BuA core. This behavior is similar to other types of intramolecular phase segregation, which were predicted for cylindrical brushes with a stiff backbone,[25] stretching of linear chains,[26] and hydrophobic polyelectrolytes.[27] In the inverted structure, the weaker interaction between the pS core and the mica substrate enabled partial desorption and coiling of the pS blocks, which was followed by contraction of the backbone.

The axial contraction of the inverted brushes with pS core and p*n*BuA shell, as well as the origin of the necklace morphology, will be discussed elsewhere.

Conclusion

Well-defined macromolecules can be synthesized by ATRP using the "grafting from" method and extending the established approach toward block copolymer side chains. The synthesized pBPEM-*graft*-(p*n*BuA-*block*-pS) and pBPEM-*graft*-(pS-*block*-p*n*BuA) core−shell systems consist of high molecular weight macromolecules. The molecular brush compositions along the backbone are uniform and do not depend on the side chain length. The cleaved side chains have a relatively low polydispersity $M_w/M_n = 1.2$. AFM experiments demonstrated that the molecular brushes adsorbed on mica have a wormlike structure. The nearly full extension of the main chain was ascribed to the strong interaction between the polar *n*BuA monomeric units and the polar mica substrate. The morphology of block copolymer brushes depends on the concurrent interaction between the blocks and the substrate and microphase segregation of the pS and p*n*BuA blocks within the molecule. The interplay of the interfacial interactions and entropic elasticity of the side chains resulted in a peculiar necklace-like morphology. The pS globuli became separated by p*n*BuA chain segments, which were tightly adsorbed to the substrate.

Acknowledgment. This work was financially supported by the National Science Foundation, ATRP Consortium at CMU, Deutsche Forschungsgemeinschaft (DFG, Germany), and a Humboldt Research Award for US Senior Scientists for K.M. The software for the analysis of molecular brushes was developed by D. Shirvanyants.

References and Notes

(1) Wintermantel, M.; Fischer, K.; Gerle, M.; Ries, R.; Schmidt, M.; Kajiwara, K.; Urakawa, H.; Wataoka, I. *Angew. Chem., Int. Ed. Engl.* **1995**, *34*, 1472.
(2) Birshtein, T. M.; Borisov, O. V.; Zhulina, E. B.; Khokhlov, A. R.; Yurasova, T. A. *Polym. Sci. USSR* **1987**, *29*, 1293.
(3) Fredrickson, G. *Macromolecules* **1993**, *26*, 2825.
(4) Subbotin, A.; Saariaho, M.; Ikkala, O.; ten Brinke, G. *Macromolecules* **2000**, *33*, 3447.
(5) Ahrens, H.; Hugenberg, N.; Schmidt, M.; Helm, C. A. *Phys. Rev. E* **1999**, *60*, 4360.
(6) Gerle, M.; Fischer, K.; Roos, S.; Müller, A. H. E.; Schmidt, M.; Sheiko, S. S.; Prokhorova, S.; Möller, M. *Macromolecules* **1999**, *32*, 2629.
(7) Sheiko, S. S.; Prokhorova, S. A.; Beers, K.; Matyjaszewski, K.; Potemkin, I. I.; Khokhlov, A. R.; Möller, M., submitted to *Macromolecules*.
(8) Tsukahara, Y.; Tsutsumi, K.; Yamashita, Y.; Shimada, S. *Macromolecules* **1990**, *23*, 5201.
(9) Yamada, K.; Miyazaki, M.; Ohno, K.; Fukuda, T.; Minoda, M. *Macromolecules* **1999**, *32*, 290.
(10) Wintermantel, M.; Gerle, M.; Fischer, K.; Schmidt, M. *Macromolecules* **1996**, *29*, 978.
(11) Ruokolainen, J.; Saariaho, M.; Ikkala, O.; ten Brinke, G.; Thomas, E. L.; Torkkeli, M.; Serimaa, R. *Macromolecules* **1999**, *32*, 1152.
(12) Djalali, R.; Hugenberg, N.; Fischer, K.; Schmidt, M. *Macromol. Rapid Commun.* **1999**, *20*, 444.
(13) Schappacher, M.; Deffieux, A. *Macromolecules* **2000**, *33*, 7371.
(14) O'Donnell, P. M.; Brzezinska, K.; Wagener, K. B. *Polym. Prepr. (Am. Chem. Soc., Div. Polym. Chem.)* **1999**, *40*, 138.
(15) Beers, K. L.; Gaynor, S. G.; Matyjaszewski, K.; Sheiko, S. S.; Möller, M. *Macromolecules* **1998**, *31*, 9413.
(16) Beers, K. L.; Gaynor, S. G.; Matyjaszewski, K.; Sheiko, S. S.; Prokhorova, S. A.; Möller, M. *Polym. Prepr. (Am. Chem. Soc., Div. Polym. Chem.)* **1999**, *40*, 446.
(17) Wang, J. S.; Matyjaszewski, K. *J. Am. Chem. Soc.* **1995**, *117*, 5614.
(18) Patten, T. E.; Matyjaszewski, K. *Adv. Mater.* **1998**, *10*, 901.
(19) Beers, K. L.; Boo, S.; Gaynor, S. G.; Matyjaszewski, K. *Macromolecules* **1999**, *32*, 5772.
(20) Keller, R. N.; Wycoff, W. M. *Inorg. Synth.* **1946**, *2*, 1.
(21) Matyjaszewski, K.; Patten, T. E.; Xia, J. *J. Am. Chem. Soc.* **1997**, *119*, 674.
(22) $M_{\text{rep.unit}} = M(\text{BPEM}) + n \times M(\text{side-chain monomer})$; $[\text{In}] = m_{\text{polymer}}/M_{\text{rep unit}}$.
(23) Polydispersity dependence of multiarm star molecules: $M_w/M_n = 1 + (1/f)$, where f is the functionality of the star. Schaefgen, J. R.; Flory, P. J. *J. Am. Chem. Soc.* **1948**, *70*, 2709.
(24) Acar, A. E.; Yagci, M. B.; Mathias, L. J. *Macromolecules* **2000**, *33*, 7700.
(25) Williams, D. R. M. *J. Phys. II* **1993**, *3*, 1313.
(26) Halperin, A.; Zhulina, E. B. *Europhys. Lett.* **1991**, *15*, 417.
(27) Dobrynin, A. V.; Rubinstein, M.; Obukhov, S. P. *Macromolecules* **1996**, *29*, 2974.

MA010001R